A EUROPEAN JOURNAL OF CHEMICAL BIOLOGY

CHEMBIOCHEM

SYNTHETIC BIOLOGY & BIO-NANOTECHNOLOGY

Accepted Article

Title: Ascorbate oxidase mimetic activity of cupric oxide nanoparticles

Authors: Shao-Bin He, Ai-Ling Hu, Quan-Quan Zhuang, Hua-Ping Peng, Hao-Hua Deng, Wei Chen, and Guo-Lin Hong

To be cited as: *ChemBioChem* 10.1002/cbic.201900595

Link to VoR: http://dx.doi.org/10.1002/cbic.201900595

A Journal of ChemPubSoc Europe

WILEY-VCH www.chembiochem.org

ARTICLE WILEY-VCH

Ascorbate oxidase mimetic activity of cupric oxide nanoparticles

Shao-Bin He,[#a] Ai-Ling Hu,[#a,b] Quan-Quan Zhuang,[a] Hua-Ping Peng,[a] Hao-Hua Deng,*[a] Wei Chen,*[a] and Guo-Lin Hong*[c]

Abstract: Although oxidase mimetic nanozymes have been widely investigated, specific biological molecules have rarely been explored as substrates, especially for ascorbate oxidase (AAO) mimetic nanozymes. Herein, for the first time, we demonstrate that cupric oxide nanoparticles (CuO NPs) exhibit as a catalyst toward the oxidation of ascorbic acid (AA) by dissolved O_2 as a green oxidant to form dehydroascorbic acid (DHAA), thus revealing a new kind of AAO mimic. Under neutral conditions, Michaelis–Menten constant of CuO NPs (0.1302 mM) is similar to that of AAO (0.0840 mM). Furthermore, the robustness of CuO NPs is greater than that of AAO rendering them suitable for applications under various conditions. As a demonstration, a fluorescence AA sensor was established based on AAO mimetic activity of CuO NPs. To obtain a fluorescent product, o-phenylenediamine (OPDA) was used to react with DHAA produced by CuO NP-catalyzed oxidation of AA. The fabricated sensor was cost-effective, easy to fabricate, and exhibited high selectivity/sensitivity with a wide linear range (1.25×10^{-6} to 1.125×10^{-4} M) and a low limit of detection (3.2×10^{-8} M). The results are expected to aid in expanding the applicability of oxidase mimetic nanozymes in a variety of fields such as biology, medicine, and detection science.

Introduction

Over the last decade, various nanozymes (nanomaterials with intrinsic enzyme mimetic activities) have been found that successfully mimic natural enzymes.[1] Among them, peroxidase nanozyme, which uses H_2O_2 as electron acceptor, has attracted the most attention due to its wide application. However, in some applications, the addition of H_2O_2 is undesirable owing to its instability and destructive nature. Therefore, it is desirable to develop oxidase mimics that can catalyze oxidation reactions using O_2 as green oxidant. Asati and co-workers showed for the first time that CeO_2 nanoparticles (NPs) possess oxidase mimetic activity.[2] Subsequent efforts have explored other nanozymes with oxidase activity, including Au, Ag, Pt, Au@Pt, Au@Ag, and Au@Pd/Pt.[3] Although these types of nanomaterials have excellent oxidase mimetic activity, their widespread application has been prohibited by poor substrate selectivity. Up to now, most substrates for oxidase mimetic nanozymes have been non-specific model substrates (e.g., 3,3',5,5'-tetramethylbenzidine, *o*-phenylenediamine (OPDA), 2, 2'-azino-bis(3-ethylbenzothiazoline-6-sulfonic acid)).[4] However, few studies have examined specific biological molecules as substrates.[5] Hence, the exploration of nanozymes that catalyze specific biomolecular substrates is highly desirable.

Cu-based materials have been studied extensively owing to its special properties and extensive applications in cross-coupling catalysis, immunoassays, high-temperature superconductor, antimicrobial applications, biosensors, and field-emission emitters.[6] Furthermore, our earlier work revealed water-soluble cupric oxide nanoparticles (CuO NPs) to have intrinsic enzyme mimetic activity, igniting widespread interest in the application of these promising nanozymes to replace enzymes.[7] Notably, self-cascade reactions catalyzed by CuO NPs with specific biological molecules (e.g. cysteine and glutathione) allowed oxidase and peroxidase mimetic activities to be established for the efficient detection of cysteine, glutathione, and Ag^+, providing a new design concept for the use of CuO NPs.[8] These studies suggest that further exploration of the oxidase-like activities of CuO NPs toward specific biological molecules would broaden their applications and provide insight into the nanozyme-based catalytic mechanism.

Ascorbate oxidase (AAO), a multi-copper enzyme, catalyzes the reduction of O_2 into water with synchronized oxidation of ascorbic acid (AA).[9] Mertz and co-workers reported an apparent correlation between the enzyme activity of AAO and cell enlargement in maize root cells, with the enzyme activity of AAO mainly associated with the cell wall fraction.[10] Furthermore, it has been suggested that AAO could be a important role in dynamic system for oxygen management in plants and regulate the growth of plant cells by working in accordance with AA.[11] However, the potential applicability of AAO in the fields of biomedicine, biosensor, and biotechnology is not yet fully understood. Similar to some other natural enzymes, AAO has some serious disadvantages such as a low thermal stability, a high cost, and tedious preparation/purification processes.[12] It's should be noted that few studies have investigated the ascorbate oxidase mimetic activity of nanomaterials.[3d,13] Thus efforts are required to obtain enzyme mimetics for AAO.

Herein, we found that CuO NPs possess AAO mimetic activity, catalyzing the oxidation of AA to dehydroascorbic acid (DHAA) in the presence of O_2, and the good AAO mimetic activity and stability of CuO NPs makes them suitable for various applications. To demonstration the applicability of CuO NPs, a fluorescence sensor for AA detection was established based on CuO NP-catalyzed AA oxidation and DHAA-induced formation of fluorescent 3-(1, 2-dihydroxyethyl) furo[3,4-b]quinoxaline-1-one (DFQ) from non-fluorescent OPDA.[14] After optimizing the detection response, this simple, low-cost, selective, and sensitive fluorometric method yielded satisfactory results for the

[a] Prof. W. Chen, Dr. S.B. He, A.L. Hu, Dr. Q.Q. Zhuang, Prof. H.P. Peng, Prof. H.H. Deng
Department of Pharmaceutical Analysis
Fujian Medical University
Fuzhou 350004, China
E-mail: chenandhu@163.com, DHH8908@163.com (H.H. Deng)
[b] A.L. Hu
Department of Pharmacy, First Hospital of Qinhuangdao, Qinhuangdao 066000, China
[c] Prof. G.L. Hong
Department of Laboratory Medicine
The First Affiliated Hospital of Xiamen University
Xiamen 361003, China
18860089899@139.com (G.L. Hong)
* Corresponding author. Tel./fax: +86 591 22862016.
# These authors contributed equally to this work.

Supporting information for this article is given via a link at the end of the document.

quantitative sensing of AA in real samples. These investigations of AAO mimetic activity of CuO NPs enrich the family of oxidase mimetic nanozymes and provide the opportunity to expand their applications in biology, medicine, and detection science.

Results and Discussion

CuO NPs were prepared via a previously reported quick-precipitation method.[7b] The morphology and particle size of the as-prepared CuO NPs were characterized by TEM (Fig. 1A). The TEM image in Fig. 1A revealed that CuO NPs consists of spherical particles with a uniform morphology. The size distribution analysis was adjusted by Gaussian distribution and the result revealed CuO NPs with an average diameter of approximately 6.8 nm (Fig. 1B). A typical XRD pattern of CuO NPs was also indicated in Fig. 1C. It could be noted that the matrix of these NPs is indexed as a CuO phase with a monoclinic structure (Lattice constants: a = 4.68 Å, b = 3.42 Å, c = 5.13 Å, and β = 99.54°, *JCPDS No. 72-0629*). Moreover, no obvious impurity peaks were found confirming the high phase purity of the obtained CuO NPs. The diffraction pattern of CuO NPs has broadened peaks ascribed to the small particle size which is in agreement with the result from the TEM image.

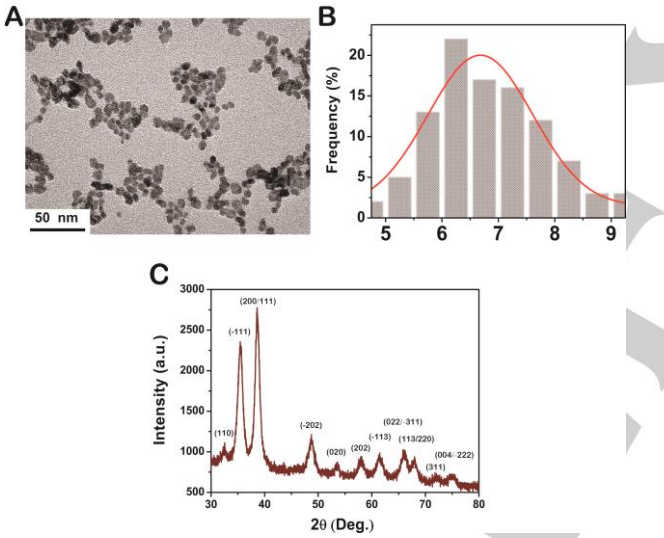

Figure 1. (A) TEM image of CuO NPs. (B) Size distribution analysis (100 random NPs) of CuO NPs. (C) XRD pattern of CuO NPs.

The oxidation of AA as catalyzed by CuO NPs in dissolved O_2 was monitored by recording the absorption at 265 nm using UV/Vis spectroscopy (Fig. 2A). AA exhibits a distinct absorption maximum at 265 nm (trace a). However, when CuO NPs were incubated with AA, an obvious decrease of absorbance at 265 nm was noted, demonstrating that AA was consumed in reaction (trace b). Moreover, experiments under de-oxygenated conditions (trace c) supported the involvement of O_2 in the reaction because no significant decrease in the absorbance at 265 nm was observed when N_2 was bubbled.

To obtain insight into the catalytic process of the AA-O_2-CuO NPs reaction, high-performance liquid chromatography analyses were performed and chromatographs depicting AA, DHAA, and AA-O_2-CuO NPs are shown in Fig. 2B. Notably, when monitoring at 265 nm, a strong peak was observed for AA (trace a) but a poor response was obtained for DHAA (trace b), and the products of the AA-O_2-CuO NPs reaction could not be observed (trace c) using a C_{18} column with methanol-KH_2PO_4 (0.05 M, pH = 6) as the mobile phase. Monitoring at 210 nm revealed that AA eluted at 3 min (trace d), whereas DHAA eluted at 3.6 min (trace e). Meanwhile, the addition of CuO NPs to AA (trace f) resulted in a remarkable decrease in the peak at 3 min and the appearance of a peak at 3.6 min, which indicated that AA can be oxidized to DHAA by O_2 in the presence of CuO NPs.

Fig. 2C depicts the time-dependent (0–180 s) changes in the absorption spectra upon oxidation of AA by O_2 in the presence of CuO NPs. The absorbance band of AA at 265 nm decreases, completely disappearing after 180 s, demonstrates that CuO NPs quickly catalyze the oxidation of AA to DHAA. To determine whether AA interacts with CuO NPs or Cu^{2+} leached from the CuO NPs under the examined reaction conditions, Cu^{2+} was obtained by incubating CuO NPs in the reaction buffer for 30 min and then removing CuO NPs from the solution by the use of centrifugation. As shown in Fig. 2D, changing rate at 265 nm increases sequential during the reaction process in the presence of CuO NPs. However, there is not any marked change in the changing rate at 265 nm when Cu^{2+} solution was used instead of the CuO NPs under the same reaction conditions. These results indicate that the ascorbate oxidase mimetic activity can be attributed to CuO NPs rather than Cu^{2+}. Hence, it can draw a conclusion that CuO NPs have AAO mimetic activity that can catalyze the oxidation of AA to DHAA in the presence of O_2.

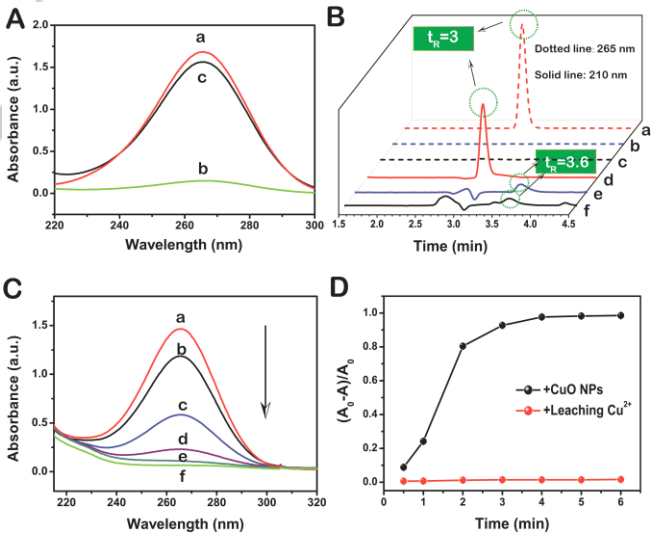

Figure 2. (A) UV/Vis spectra of (a) AA, (b) AA-O_2-CuO NPs, and (c) AA-CuO NPs under a N_2 atmosphere for 20 min. (B) Chromatogram at 265 nm of (a) AA, (b) DHAA, and (c) AA-O_2-CuO NPs, and chromatograms at 210 nm of (d) AA, (e) DHAA, and (f) AA-O_2-CuO NPs (t_R is the abbreviation of retention time). (C) Time-dependent spectral changes (a, 0 s; b, 30 s; c, 60 s; d, 120 s; e, 180 s) of AA corresponding to CuO NP-catalyzed oxidation (f, solution containing DHAA instead of AA). (D) Evolution of the time-dependent absorbance-changing rate at 265 nm for AA in the presence of (a) CuO NPs and (b) leaching solution (Cu^{2+}).

To further evaluate the ascorbate oxidase mimetic activity of CuO NPs, the effects of the concentration of CuO NPs, pH, and temperature on the AA-O_2-CuO NPs system were investigated by recording the absorption (265 nm) using UV/Vis spectroscopy. Fig. 3A shows the relationship between the changing rate of AA at 265 nm and CuO NPs concentration. The changing rate increases until the concentration of CuO NPs reaches 0.5 mg/L and then remains approximately constant at higher CuO NP concentrations. The stability of ascorbyl radicals is known to vary with reaction conditions such as pH and temperature. In this case, the optimal pH and temperature were observed to be approximately 7.0–9.0 (Fig. 3B) and 40–60 °C (Fig. 3C), respectively. Thus, we employed pH 7.0 and 45 °C as the optimal conditions in subsequent experiments.

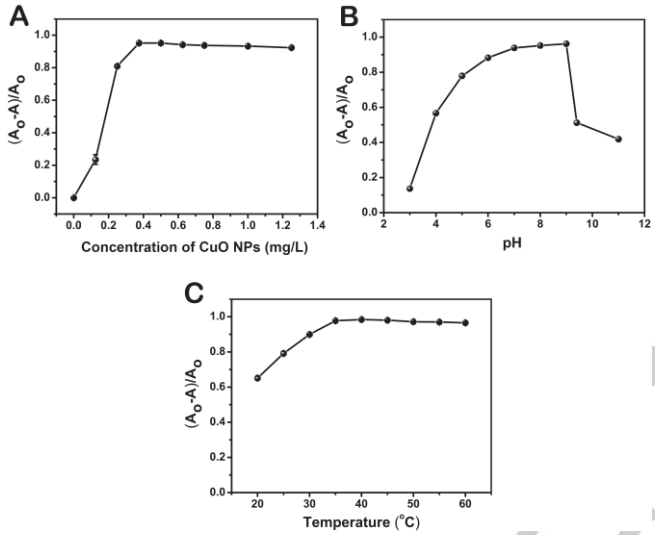

Figure 3. Effects of (A) concentration of CuO NPs, (B) pH, and (C) temperature on the absorbance-changing rate of the AA-O_2-CuO NPs system.

To obtain the steady-state kinetic parameters, we further studied the catalytic behavior of CuO NPs and AAO with AA as substrate, built on enzyme kinetics theory and methods. The Michaelis–Menten model is one of the most widely used models and most commonly used to study enzymatic reaction. In Fig. 4, the solid circles are the experimental data and the solid curves are fits to the Michaelis–Menten model. In a range of AA concentration, Michaelis–Menten equations were achieved for CuO NPs (Fig. 4A) and AAO (Fig. 4B), and the Michaelis–Menten constant (K_m) can be obtained. The kinetics of the enzyme reaction can be characterized by the parameters K_m and catalytic rate constants (K_{cat}).Under a neutral condition, the K_m of CuO NPs (0.1302 mM) is slightly higher than that of AAO (0.0840 mM). The catalytic performance of CuO NPs could be attributed to their full surface exposure of CuO atoms. In order to effectively compare the catalytic behavior of CuO NPs and AAO, the catalytic rate constants (K_{cat}) of CuO NPs (26.98 s^{-1}) and AAO (363.13 s^{-1}) were calculated, respectively. These relatively minor differences in kinetic parameters demonstrate that CuO NPs and AAO possess comparable affinities for AA (Table 1).

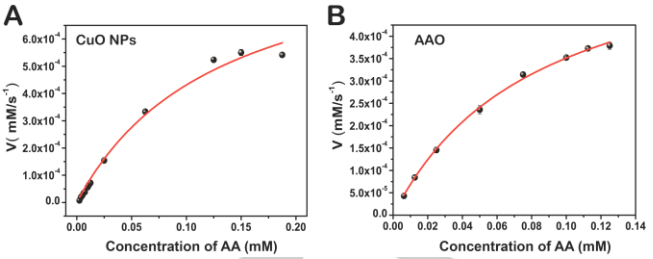

Figure 4. Steady-state kinetic assays with (A) CuO NPs and (B) AAO.

Table 1 Comparison of steady-state kinetic parameters of CuO NPs and AAO.

Catalyst	K_m (mM)	V_{max} (10^{-4} mM/s)	[E] (10^{-5} mM)	K_{cat} (s^{-1}) [a]
CuO NPs	0.1302	9.9	3.67	26.98 [b]
AAO	0.0840	6.5	0.179	363.13

[a] $K_{cat} = V_{max} / [E]$, where [E] is the concentration of the catalyst.

[b] See the calculation details in the Supporting Information.

As an inorganic material, CuO NPs are expected to be stable under harsh environments over a much longer time than AAO, which tends to lose its catalytic activity after exposure to extreme pH and high temperatures. To highlight the superiority of stability of CuO NPs, the catalytic activities of CuO NPs and AAO were tested after incubation at a range of pH values and temperatures for 1 h. After treatment at a pH lower than 5 or higher than 9 (Fig. 5A) or temperatures greater than 40 °C (Fig. 5B), the catalytic activity of AAO decreased obviously. Unlike AAO, CuO NPs were stable over a wide range of pH values (3–12, Fig. 5A) and temperatures (10–90 °C, Fig. 5B). Taken together, the robust stability and considerable ascorbate oxidase mimetic activity makes CuO NPs suitable for analytical applications.

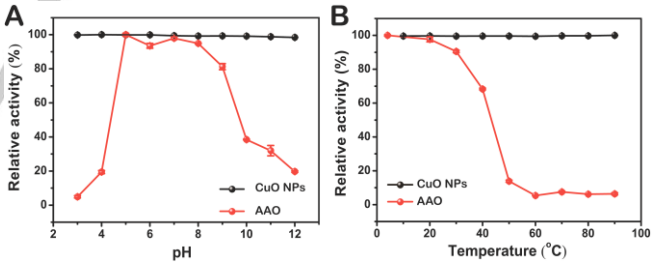

Figure 5. Relative activities of CuO NPs and AAO after incubation for 1 h at various (A) pH values and (B) temperatures.

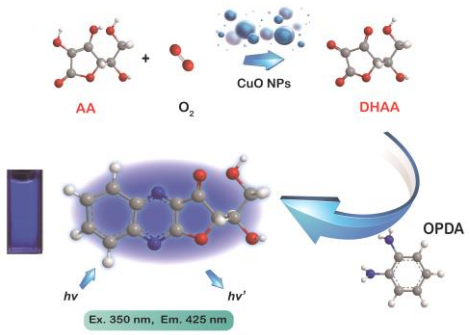

Scheme 1. Schematic illustration of the ascorbate oxidase mimetic activity of CuO NPs and OPDA as a probe for fluorescence sensing of AA.

For sensing of AA, OPDA can be used as a probe for the final product (DHAA) of the reaction of the AA-O_2-CuO NPs system. OPDA is non fluorescent, but the specific reaction between OPDA and DHAA produces DFQ, which is strong fluorescent. Thus using the AAO mimetic activity of CuO NPs, AA can be rapidly oxidized by dissolved O_2 to DHAA, which then reacts with OPDA to produce DFQ, thus providing a unique method for AA sensing (Scheme 1). As is illustrated in Fig. 6, both the OPDA-O_2 (trace a) and OPDA-O_2-CuO NPs system (trace b) exhibit almost no fluorescence intensity. Although AA can undergo auto-oxidation in the absence of a catalyst, only weak fluorescence was observed in OPDA-O_2-AA system (trace c), whereas the fluorescence intensity of the OPDA-AA-O_2-CuO NPs system (trace d) was greatly enhanced, with an emission maximum at 425 nm when excited at 350 nm. The fluorescence spectrum of the OPDA-AA-O_2-CuO NPs system (trace d) is similar in shape to that of OPDA-DHAA system (Fig. S1), which confirms that OPDA reacts directly with DHAA obtained by the Cu NP-catalyzed oxidation of AA. The inset photograph in Scheme 1 clearly shows luminescence of the OPDA-AA-O_2-CuO NPs system under a UV lamp.

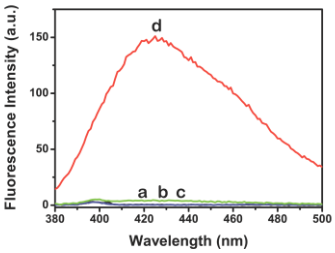

Figure 6. Fluorescence emission spectra of (a) OPDA, (b) OPDA-CuO NPs, (c) OPDA-AA, and (d) OPDA-AA-CuO NPs (excitation wavelength = 350 nm).

The OPDA-AA-O_2-CuO NPs system was subsequently optimized to establish the optimum analytical conditions for AA sensing (Fig. S2). The effect of OPDA concentration was tested in the range from 6.25 × 10^{-3} to 0.625 mM and the maximum fluorescence intensity was observed at 0.25 mM of OPDA, which could be chosen as the optimum concentration for further experiments (Fig. S2A). The effect of pH in reaction solution was examined by adjusting the pH from 3 to 9. As shown in Fig. S2B, the fluorescence intensity remains approximately constant at pH from 3–6 and then decreases dramatically from pH 6.5 to pH 9. Therefore, pH 5.0 was selected as the optimum pH for further experiments. Fig. S2C shows that the fluorescence intensity increased significantly as the incubation temperature increased to 20 °C. Slight variations were observed in the fluorescence intensity at temperature of 20–30 °C, and then the fluorescence intensity decreased gradually above 30 °C. Therefore, 30 °C was selected as the reaction temperature for further experiments. The kinetics of reaction between DHAA and OPDA to produce a fluorescence signal was also investigated (Fig. S2D). Initially, the signal increases, with a maximum fluorescence obtained at 20 min. Hence, reaction time of 20 min was chosen for further experiments.

Fig. 7A depicts the fluorescence response of OPDA-AA-O_2-CuO NPs system in the presence of AA concentration. Under optimal reaction conditions, the fluorescence intensity at 425 nm was proportional to the AA concentration in the range of 1.25 × 10^{-6} to 1.125 × 10^{-4} M with a low limit of detection (LOD) of 3.2 × 10^{-8} M (Fig. 7B). The RSD was 1.8% at 1.125 × 10^{-4} M AA (n = 6). The analytical performance of this OPDA-AA-O_2-CuO NPs sensor was compared with that of typical AA detection methods reported in recent years (Table 2). Compared with these other methods, the approach proposed herein shows a wider linear range, better sensitivity, and relatively low detection limits.

To confirm the selectivity of this method for AA, experiments were conducted using cysteine, homo-cysteine, GSH, glucose, lactose, maltose, fructose, citric acid, and uric acid (Fig. 7C). A high intensity was obtained in the presence of AA, whereas no obvious signals were observed for the other compounds, even though their concentrations (1.25 mM) were 10-fold higher than that of AA (0.125 mM). By combining the CuO NP-catalyzed oxidation of AA with the selectivity of OPDA for DHAA, the system achieved high selectivity for AA.

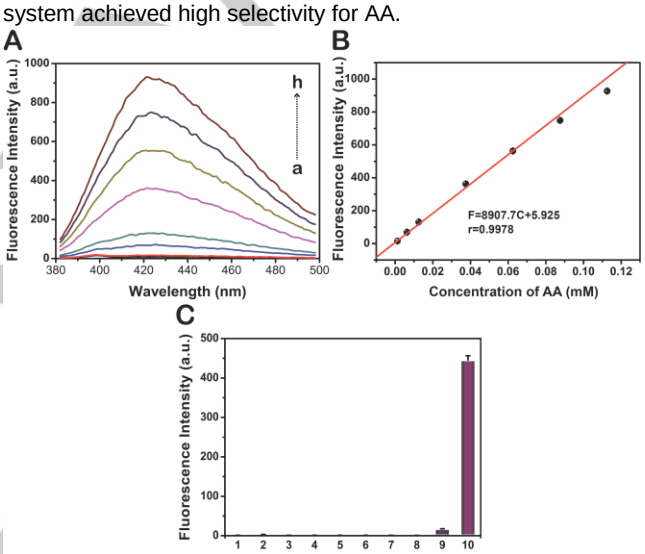

Figure 7. (A) Fluorescence emission spectra (excitation wavelength = 350 nm) of the OPDA-AA-O_2-CuO NPs system at different AA concentrations (10^{-6} M): (a) 0, (b) 1.25, (c) 6.25, (d) 12.5, (e) 37.5, (f) 62.5, (g) 87.5, and (h) 112.5. (B) Calibration plot constructed using the fluorescence intensity at 425 nm. (C) Fluorescence intensities (at 425 nm) of OPDA-CuO NPs in the presence of foreign substances: 1, cysteine; 2, homocysteine; 3, GSH; 4, glucose; 5, lactose; 6, maltose; 7, fructose; 8, citric acid; 9, uric acid; 10, AA (1-9: 1.25 mM; 10: 0.125 mM).

To explore the applicability and feasibility of the developed sensing method, it was applied to the determination of AA in real samples such as commercial Vitamin C tablets and a lemon beverage. As shown in Table 3, results obtained using the OPDA-AA-O_2-CuO NPs sensor were in good agreement with those determined using the Standard Chinese Pharmacopoeia Iodimetric method (standard method). The practical applicability of the OPDA-AA-O_2-CuO NPs biosensor was verified through standard addition experiments. The RSD was less than 5.0% and the average recovery of real samples was between 92.6% and 110.6%. These results indicate that the OPDA-AA-O_2-CuO NPs sensor meets the requirements for microanalysis and is practical for the determination of AA in commercial tablets and lemon beverages. Moreover, both the F-test and t-test showed

no significant statistical difference at the 95% confidence level between the proposed and standard analytical methods.

Table 2 Comparison of typical methods for AA sensing.

Method	Linear range (M)	LOD (M)	Ref.
Cyclic voltammetry	2×10^{-6} to 2.06×10^{-4}	9×10^{-7}	15
	1.2×10^{-6} to 1.61×10^{-3}	4.3×10^{-7}	16
Amperometry	5×10^{-5} to 2×10^{-2}	1.5×10^{-6}	17
Colorimetry	6×10^{-6} to 8×10^{-5}	8×10^{-7}	18
	2×10^{-6} to 5×10^{-5}	1.6×10^{-7}	19
	1×10^{-7} to 2.5×10^{-6}	4.9×10^{-8}	20
	1×10^{-5} to 1×10^{-3}	1.4×10^{-6}	21
	0 to 5×10^{-5}	4×10^{-8}	22
	5×10^{-6} to 3×10^{-5}	3.6×10^{-6}	23
	1.5×10^{-6} to 1×10^{-5}	2×10^{-7}	24
Fluorescence	3×10^{-5} to 1.0×10^{-4}	-	25
	-	2×10^{-6}	26
OPDA-AA-O_2-CuO NPs	1.25×10^{-6} to 1.125×10^{-4}	3.2×10^{-8}	This work

Table 3 Analytical results for AA contents of samples determined using the OPDA-AA-O_2-CuO NPs sensor and the standard method.

Sample	Proposed method	Standard method	F-test	t-test
Vitamin C tablets (mg)	5.8 ± 0.18	5.5 ± 0.28	2.4	0.5
	7.1 ± 0.33	7.2 ± 0.26	1.6	0.1
Lemon-beverage (mM)	3.08 ±0.12	3.33 ± 0.15	1.6	1.0

$F_{0.05,2,2} = 19.00$, $t_{0.05,4} = 2.776$, n = 3

Conclusions

In conclusion, CuO NPs exhibited as a catalyst toward the oxidation of AA by O_2 as a green oxidant to form DHAA under mild conditions. The apparent steady-state kinetic parameters indicated that this new type of ascorbate oxidase mimic and AAO have similar affinities for AA, whereas CuO NPs catalyze the oxidation reaction more rapidly than AAO. Moreover, CuO NPs exhibited considerable stability and almost constant catalytic activity over a wide range of storage pH and temperature. By coupling the CuO NP-catalyzed oxidation of AA to the reaction between OPDA and DHAA, which produces a fluorescent product, a sensitive/selective assay for AA was realized with a lowest detection limit of 3.2×10^{-8} M. In addition, this proposed method was successfully applied to determine AA in real samples. Owing to the excellent ascorbate oxidase mimetic activity of CuO NPs, there is considerable scope for improving their enzyme mimetic activity and exploring their potential applications in biology, medicine, and detection science.

Experimental Section

Cupric acetate, H_2O_2 (30wt%), AA, glucose, maltose, D-fructose, L-cysteine, uric acid, citric acid, oxalic acid, ethanol, NaCl, GSH, lactose, sodium hydroxide, and OPDA were purchased from Sinopharm Chemical Reagent Co. Ltd. (China). DHAA and AAO were purchased from Sigma Co. Ltd. (Germany).

Transmission electron microscopy (TEM) images were collected with a JEM-2100 TEM (JEOL, Japan). X-ray diffraction (XRD) patterns were recorded with a Bruker D8 Advance diffractometer. A UV-2450 spectrophotometer (Shimadzu, Japan) was used to record the UV/Vis absorption spectra. High-performance liquid chromatography analyses were performed using an HPLC-1200 instrument (Agilent Technologies, USA). A Cary Eclipse fluorescence spectrometer (Agilent Technologies, USA) was used to record the fluorescence spectra.

CuO NPs were prepared via a previously reported quick-precipitation method.[7b] In order to investigate the ascorbate oxidase mimetic activity of the CuO NPs, catalytic oxidation of AA in the presence of O_2 was conducted. Typically, an experiment was carried out at 45 °C by using 0.5 mg/L CuO NPs in a reaction volume of 4.0 mL (200 mM phosphate buffer, pH = 7.0) with 500 µL of 0.125 mM AA as substrates. Then, the products were monitored at λ = 265 nm using UV/Vis spectroscopy. To test the stability, the CuO NPs were incubated at different temperatures (10–90 °C) or pH values (3–12) for 1 h, and then their ascorbate oxidase mimetic activities were measured under the standard conditions mentioned above.

First, 500 µL of AA of various concentrations and 50 µL of 40 mg/L CuO NPs were added into 450 µL of phosphate buffer solution (200 mM, pH 7.0). After incubating at 40 °C for 6 min, 2.5 mL of phosphate buffer solution (200 mM, pH 5.0) and 500 µL of 2 mM OPDA were added, and the resulting mixture was incubated for another 20 min at 30 °C. The fluorescence spectra of the resulting reaction solution were recorded at an excitation wavelength of 350 nm.

For the pharmaceutical analysis of AA, samples of vitamin C tablets were dissolved and diluted 10-fold in purified water after centrifugation, and analyzed directly. The lemon beverage samples were diluted (1:10 v/v) to obtain an AA concentration within the linear range of response. For AA analysis, results of the proposed method were compared with those of the *Standard Chinese Pharmacopoeia Iodimetric* method.

Acknowledgements

The authors gratefully acknowledge the financial support of the National Natural Science Foundation of China (21175023), the Program for Innovative Leading Talents in Fujian Province (2016B016), and the Program for Innovative Research Team in Science and Technology in Fujian Province University (2018B033).

Keywords: Cupric oxide nanoparticles • ascorbate oxidase mimetic activity • ascorbic acid • *o*-phenylenediamine • fluorometric sensor

[1] (a) H. Wei, E. Wang, *Chem. Soc. Rev.*, **2013**, *42*, 6060–6093; (b) J. Wu, X. Wang, Q. Wang, Z. Lou, S. Li, Y. Zhu, L. Qin, H. Wei, *Chem. Soc. Rev.* **2019**, *48*, 1004-1076; (c) L. Gao, J. Zhuang, L. Nie, J. Zhang, Y. Zhang, N. Gu, T. Wang, J. Feng, D. Yang and S. Perrett, *Nat. Nanotechnol.* **2007**, *2*, 577; (d) Z. Zhang, X. Zhang, B. Liu, J. Liu, *J. Am. Chem. Soc.* **2017**, *139*, 5412-5419; (e) X. Shen, W. Liu, X. Gao, Z. Lu, X. Wu, X. Gao, *J. Am. Chem. Soc.* **2015**, *137*, 15882-15891; (f) H. H. Deng, X. L. Lin, Y. H. Liu, K. L. Li, Q. Q. Zhuang, H. P. Peng, A. L. Liu, X. H. Xia, W. Chen, *Nanoscale* **2017**, *9*, 10292-10300; (g) S. B. He, H. H. Deng, A. L. Liu, G. W. Li, X. H. Lin, W. Chen, X. H. Xia, *ChemCatChem* **2014**, *6*, 1543-1548; (h) H. Liang, F. Lin, Z. Zhang, B. Liu, S. Jiang, Q. Yuan. J. Liu, *ACS Appl. Mater. Interfaces* **2017**, *9*, 1352-1360; (i) Y. Yoshihisa, Q. L. Zhao, M. A. Hassan, Z. L. Wei, M. Furuichi, Y. Miyamoto, T. Kondo, T. Shimizu, *Free Radical Res*. **2011**, *45*, 326-335; (j) S. B. He, G. W. Wu, H. H. Deng, A. L. Liu, X. H. Lin, X. H. Xia, W. Chen, *Biosens. Bioelectron.* **2014**, *62*, 331-336. (k) T. Hou, T. X. Zhao, W. Li, F. Li, P. P. Gai, *J. Mater. Chem. B* **2017**, *5*, 4607-4613.

[2] A. Asati, S. Santra, C. Kaittanis, S. Nath, J. M. Perez, *Angew. Chem. Int. Ed.* **2009**, *121*, 2344-2348.

[3] (a) W. Luo, C. Zhu, S. Su, D. Li, Y. He, Q. Huang, C. Fan, *ACS Nano* **2010**, *4*, 7451-7458; (b) G. L. Wang, X. F. Xu, L. H. Cao, C. H. He, Z. J. Li, C. Zhang, *RSC Adv*. **2014**, *4*, 5867-5872; (c) C. J. Yu, T. H. Chen, J. Y. Jiang, W. L. Tseng, *Nanoscale* **2014**, *6*, 9618-9624; (d) J. Liu, X. Hu, S. Hou, T. Wen, W. Liu, X. Zhu, J. J. Yin, X. Wu, *Sens. Actuat. B-Chem.* **2012**, *166*, 708-714; (e) L. Wang, Y. Zeng, A. Shen, X. Zhou, J. Hu, *Chem. Commun.* **2015**, 51, 2052-2055; (f) K. Zhang, X. Hu, J. Liu, J. J. Yin, S. Hou, T. Wen, W. He, Y. Ji, Y. Guo, Q. Wang, *Langmuir* **2011**, *27*, 2796-2803.

[4] (a) X. Liu, Q. Wang, H. Zhao, L. Zhang, Y. Su, Y. Lv, *Analyst* **2012**, *137*, 4552-4558; (b) J. Liu, X. Hu, S. Hou, T. Wen, W. Liu, X. Zhu, X. Wu, *Chem. Commun.* **2011**, *47*, 10981-10983; (c) X. Zhang, X. Mao, S. Li, W. Dong, Y. Huang, *Sens. Actuat. B-Chem.* **2018**, *258*, 80-87.

[5] (a) H. Zhang, X. Liang, L. Han, F. Li, *Small* **2018**, *14*, 1803256; (b) L. Han, H. Zhang, D. Chen, F. Li, *Adv. Funct. Mater.* **2018**, *28*, 1800018.

[6] (a) S. Jammi, S. Sakthivel, L. Rout, T. Mukherjee, S. Mandal, R. Mitra, P. Saha, T. Punniyamurthy, *J. Org. Chem.* **2009**, *74*, 1971-1976; (b) C. H. Lu, Y. W. Wang, S. L. Ye, G. N. Chen, H. H. Yang, *NPG Asia Mater.* **2012**, *4*, 10; (c) T. Yang, C. M. Li, J. H. He, B. Chen, Y. F. Li, C. Z. Huang, *Anal. Chem.* **2018**, *90*, 9966-9974; (d) X. Zheng, C. Xu, Y. Tomokiyo, E. Tanaka, H. Yamada, Y. Soejima, *Phys. Rev. Lett.* **2000**, *85*, 5170; (e) G. Ren, D. Hu, E. W. Cheng, M. A. Vargas-Reus, P. Reip, R. P. Allaker, *Int. J. Antimicrob. Agent.* **2009**, *33*, 587-590; (f) J. Yang, L. C. Jiang, W. D. Zhang, S. Gunasekaran, *Talanta* **2010**, *82*, 25-33. (g) H. Y. Li, J. F. Chang, T. Hou, L. Ge, F. Li, *Talanta* **2016**, *160*, 475-480.

[7] (a) W. Chen, J. Chen, A. L. Liu, L. M. Wang, G. W. Li, X. H. Lin, *ChemCatChem*, **2011**, *3*, 1151-1154; (b) W. Chen, J. Chen, Y. B. Feng, L. Hong, Q. Y. Chen, L. F. Wu, X. H. Lin, X. H. Xia, *Analyst* **2012**, *137*, 1706-1712; (c) W. Chen, L. Hong, A. L. Liu, J. Q. Liu, X. H. Lin, X. H. Xia, *Talanta* **2012**, *99*, 643-648; (d) L. Hong, A. L. Liu, G. W. Li, W. Chen, X. H. Lin, *Biosens. Bioelectron.* **2013**, *43*, 1-5; (e) A. L. Hu, Y. H. Liu, H. H. Deng, G. L. Hong, A. L. Liu, X. H. Lin, X. H. Xia, W. Chen, *Biosens. Bioelectron.* **2014**, *61*, 374-378.

[8] (a) A. L. Hu, H. H. Deng, X. Q. Zheng, Y. Y. Wu, X. L. Lin, A. L. Liu, X. H. Xia, H. P. Peng, W. Chen, G. L. Hong, *Biosens. Bioelectron.* **2017**, *97*, 21-25; (b) L. Y. He, Y. X. Lu, X. Y. Gao, P. S. Song, Z. X. Huang, S. Liu, Y. Y. Liu, *ACS Sustain. Chem. Eng.* **2018**, *6*, 12132-12139.

[9] M. De Tullio, R. Liso, O. Arrigoni, *Biol. Plantarum* **2004**, *48*, 161-166.

[10] D. Mertz, *Am. J. Bot.* **1961**, *48*, 405-413.

[11] S. Y. Leong, I. Oey, *Food Chem.* **2012**, *134*, 2075-2085.

[12] (a) M. C. De Tullio, S. Ciraci, R. Liso, O. Arrigoni, *J. Plant Physiol.* **2007**, *164*, 39-46; (b) A. W. Munyaka, E. E. Makule, I. Oey, A. Van Loey, M. Hendrickx, *J. Food Sci.* **2010**, *75*, C336-C340.

[13] C. Chen, S. Fan, C. Li, Y. Chong, X. Tian, J. Zheng, P. P. Fu, X. Jiang, W. G. Wamer, J. J. Yin, *J. Mater. Chem. B.* **2016**, 4, 7895-7901.

[14] X. Wu, Y. Diao, C. Sun, J. Yang, Y. Wang, S. Sun, *Talanta* **2003**, *59*, 95-99.

[15] N. Chauhan, J. Narang, C. Pundir, *Analyst* **2011**, *136*, 1938-1945.

[16] C. Zhou, S. Li, W. Zhu, H. Pang, H. Ma, *Electrochim. Acta.* **2013**, *113*, 454-463.

[17] M. Liu, Y. Wen, J. Xu, H. He, D. Li, R. Yue, G. Liu, *Anal. Sci.* **2011**, *27*, 477-477.

[18] H. M. NEZHAD, M. Karimi, F. Shahheydari, *Sci. Iran.* **2010**, *17*, 148-153.

[19] X. H. Yang, J. Ling, J. Peng, Q. E. Cao, L. Wang, Z. T. Ding, J. Xiong, *Spectrochim. Acta. A.* **2013**, 106, 224-230.

[20] G. Wang, Z. Chen, L. Chen, *Nanoscale* **2011**, *3*, 1756-1759.

[21] H. Tan, C. Ma, L. Gao, Q. Li, Y. Song, F. Xu, T. Wang, L. Wang, *Chem. Eur.-J.* **2014**, *20*, 16377–16383.

[22] Y. Z. Jiang, N. Song, C. Wang, N. Pinna, X. F. Lu, *J. Mater. Chem. B* **2017**, *5*, 5499-5505.

[23] G. Darabdhara, B. Sharma, M. R. Das, R. Boukherroub, S. Szunerits, *Sens. Actuat. B-Chem.* **2017**, *238*, 842-851.

[24] X. Wang, P. Wu, X. Hou, Y. Lv, *Analyst* **2013**, *138*, 229-233.

[25] M. Zheng, Z. Xie, D. Qu, D. Li, P. Du, X. Jing, Z. Sun, *ACS Appl. Mater. Interfaces* **2013**, *5*, 13242-13247.

[26] B. Bao, N. Tao, M. Ma, L. Zhang, L. Yuwen, Q. Fan, L. Wang, W. Huang, *Soft Mater.* **2014**, *12*, 73-78.

Entry for the Table of Contents

ARTICLE

Herein, for the first time, we demonstrate that cupric oxide nanoparticles (CuO NPs) exhibit as a catalyst toward the oxidation of ascorbic acid (AA) by dissolved O_2 as a green oxidant to form dehydroascorbic acid (DHAA), thus revealing a new kind of ascorbate oxidase (AAO) mimic. The results are expected to aid in expanding the applicability of oxidase mimetic nanozymes in a variety of fields such as biology, medicine, and detection science.

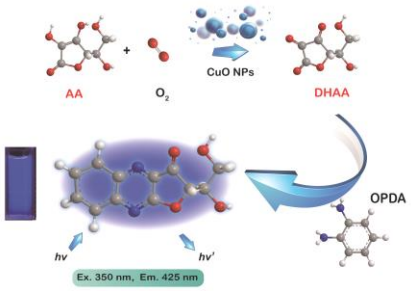

Shao-Bin He,[#[a]] Ai-Ling Hu,[#[a,b]] Quan-Quan Zhuang,[[a]] Hua-Ping Peng,[[a]] Hao-Hua Deng,*[[a]] Wei Chen,*[[a]] and Guo-Lin Hong*[[c]]

Page No. – Page No.

Ascorbate oxidase mimetic activity of cupric oxide nanoparticles